Understanding the effects of climate warming on streamflow and active groundwater storage in an alpine catchment, upper Lhasa River

Lu Lin[a,b], Man Gao[c], Jintao Liu[a,b*], Jiarong Wang[a,b], Shuhong Wang[a,b*], Xi Chen[a,b,c], Hu Liu[d]

[a] *State Key Laboratory of Hydrology-Water Resources and Hydraulic Engineering, Hohai University, Nanjing 210098, People's Republic of China*

[b] *College of Hydrology and Water Resources, Hohai University, Nanjing 210098, People's Republic of China*

[c] *Institute of Surface-Earth System Science, Tianjin University, Tianjin 300072, People's Republic of China*

[d] *Linze Inland River Basin Research Station, Chinese Ecosystem Research Network, Lanzhou 730000, People's Republic of China*

* *Corresponding author. Tel.: +86-025-83787803; Fax: +86-025-83786606.*

E-mail address: jtliu@hhu.edu.cn (J.T. Liu).

Abstract

Climate warming is changing streamflow regimes and groundwater storage in cold alpine regions. In this study, a headwater catchment named Yangbajain in the Lhasa River Basin is adopted as the study area for assessing streamflow changes and active groundwater storage in response to climate warming. The results show that both annual streamflow and mean air temperature increase significantly at rates of about 12.30 mm/10a and 0.28 °C/10a during 1979-2013 in the study area. The results of gray relational analysis indicate that the air temperature acts as a primary factor for the increased streamflow. Due to climate warming, the total glacier volume has retreated by over 25% for the past half century, and the areal extent of permafrost has degraded by 15.3% in the recent twenty years. Parallel comparisons with other sub-basins in the Lhasa River Basin indirectly reveal that the increased streamflow at the Yangbajain station is mainly fed by the accelerated glacier retreat. Through baseflow recession analysis, we also find that the estimated groundwater storage that is comparable with the GRACE data increases significantly at the rates of about 19.32 mm/10a during these years. That is to say, as permafrost thawing, more spaces have been released to accommodate the increasing meltwater. Finally, a large water imbalance ($> 5.79\times10^7$ m^3/a) between the melt-derived runoff and the actually increase of runoff as well as the groundwater storage is also observed. The results in this study suggest that due to climate warming, the impacts of glacial retreat and permafrost degradation show compound behaviors on storage-discharge mechanism,

which fundamentally affects the water supply and the mechanisms of streamflow generation and change.

Keywords: Climate warming; Streamflow; Groundwater storage; Glacier retreat; Permafrost degradation; Tibetan Plateau

1. Introduction

Often referred to as the “Water Tower of Asia”, the Tibetan Plateau (TP) is the source area of major rivers in Asia, e.g., the Yellow, Yangtze, Lancang-Mekong, Yarlu Zangbo-Brahmaputra, and Nu-Salween, Indus Rivers (Cuo et al., 2014). The delayed release of water resources on the TP through glacier melt can augment river runoff during dry periods, giving it a pivotal role for water supply for downstream populations, agriculture and industries in these rivers (Viviroli et al., 2007; Pritchard, 2017). However, the TP is experiencing a significant warming period during the last half century (Kang et al., 2010; Liu and Chen, 2000). Along with the rising temperature, major warming-induced changes have occurred over the TP, such as glacier retreat (Yao et al., 2004; Yao et al., 2007) and frozen ground degradation (Wu and Zhang, 2008; Xu et al., 2019). Hence, it is of great importance to elucidate how climate warming influences hydrological processes and water resources on the TP.

In cold alpine catchments, glacier is known as “solid reservoir” that supplies water through streamflow, while frozen ground, especially permafrost, servers as an impermeable barrier to the interaction between surface water and groundwater (Immerzeel et al., 2010; Walvoord and Kurylyk, 2016; Rogger et al., 2017). Since the 1990s, most glaciers across the TP have retreated rapidly due to global warming and caused an increase of more than 5.5% in river runoff from the plateau (Yao et al., 2007). Meltwater is the key contributor to streamflow increase especially for headwater catchments with larger glacier coverage (>5%) (Bibi et al., 2018; Xu et al.,

2019). For example, the total discharge increase by 2.7%-22.4% mainly due to the increased glacier melt that accounts for more than half of the total discharge increase in the upper Brahmaputra, i.e., Yarlu Zangbo (Su et al., 2016).

Meanwhile, in a warming climate, numerous studies suggested that frozen ground on the TP has experienced a noticeable degradation during the past decades (Cheng and Wu, 2007; Wu and Zhang, 2008; Zou et al., 2017). Frozen ground degradation can modify surface conditions and change thawed active layer storage capacity in the alpine catchments (Niu et al., 2011). Thawing of frozen ground increases surface water infiltration, supports deeper groundwater flow paths, and then enlarges groundwater storage, which is expected to have a profound effect on flow regimes (Kooi et al., 2009; Bense et al., 2012; Walvoord and Striegl, 2007; Woo et al., 2008; Ge et al., 2011; Walvoord and Kurylyk, 2016; Li et al., 2018; Wang et al., 2018). For example, Wang et al. (2018) suggested that ground ice may be a potential water source in continuous permafrost regions of central TP under global warming. However, in high mountainous regions in the TP, various terms of water recharge are quite complex especially in low elevations. In general, permafrost thawing in an arctic basin has resulted in a general upwards trend in groundwater contribution to streamflow of 0.7-0.9%/a, however, with no pervasive change in total annual runoff (Walvoord and Striegl, 2007). Similar results have also been found in the central and northern TP (Liu et al., 2011; Niu et al., 2016; Xu et al., 2019). Moreover, a slowdown in baseflow recession was found in the northeastern and central TP (Niu et al., 2011;

Niu et al., 2016; Wang et al., 2017), in northeastern China (Duan et al., 2017), and in Arctic rivers (Lyon et al., 2009; Lyon and Destouni, 2010; Walvoord and Kurylyk, 2016).

Generally, in alpine regions, climate warming by triggering glacier retreat and permafrost thawing is changing hydrological processes of storage and discharge. However, direct measurement of the changing of permafrost depth or catchment aquifer storage is still difficult to perform at catchment scale (Xu et al., 2019; Staudinger, 2017; Käser and Hunkeler, 2016). Though its resolution and accuracy is relatively low, GRACE data has always been adopted in assessing total groundwater storage changes (Green et al., 2011). More importantly, quantitatively characterizing storage properties and sensitivity to climate warming in cold alpine catchments is desired for local water as well as downstream water management (Staudinger, 2017).

Xu et al. (2019) used a simple ratio of the maximum and minimum runoff to indirectly indicate the change of storage capacity as well as the effects of permafrost on recession processes. An alternative method, namely, recession flow analysis, can theoretically be used to derive the active groundwater storage volume to reflect frozen ground degradation in a catchment (Brutsaert and Nieber, 1977; Brutsaert, 2008). For example, the groundwater storage changes can be inferred by recession flow analysis assuming linearized outflow from aquifers into streams (Lin and Yeh, 2017). Due to the complex structures and properties of catchment aquifers, the linear reservoir model may not sufficient to represent the actual storage dynamics (Wittenberg, 1999;

Chapman, 1999; Liu et al., 2016). Hence, Lyon et al. (2009) adopted the nonlinear reservoir to fit baseflow recession curves for the derivation of aquifer attributes, which can be developed for inferring aquifer storage. Buttle (2017) used Kirchner (2009) approach for estimating the dynamic storage in different basins and found that the storage and release of dynamic storage may mediate baseflow response to temporal changes. Generally, the classical recession flow analysis that is based on widely easily available hydrologic data is still widely used to provide important information on storage–discharge relationship of the basin (Patnaik et al., 2018).

In this study, the Yangbajain Catchment in the Lhasa River Basin is adopted as the study area. The catchment is experiencing glacier retreat and frozen ground degradation in response to climate warming. The main objectives of this study are (1) to assess the changes between surface runoff and baseflow in a warming climate; (2) to quantify active groundwater storage volume by recession flow analysis; (3) to analyze the impacts of the changes in active groundwater storage on streamflow variation. The paper is structured as follows. The section of Materials and Methods includes the study area, data sources and methods. The Results and Discussion sections present the changes in streamflow and its components, climate factors, and glaciers, and we will discuss the changing regimes of streamflow volume and baseflow recession in response to the changes of active groundwater storage and glaciers. The main conclusions are summarized in the section of Conclusions.

2. Materials and Methods

2.1. Study area

The 2,645 km^2 Yangbajain Catchment in the western part of the Lhasa River Basin (Figure 1a) lies between the Nyainqêntanglha Range to the northwest and the Yarlu-Zangbo suture to the south. In the central of the catchment, a wide and flat valley (Figure 1b) with low-lying terrain and thicker aquifers is in a half-graben fault-depression basin caused by the Damxung-Yangbajain Fault (Wu and Zhao, 2006; Yang et al., 2017). As a half graben system, the north-south trending Damxung-Yangbajain Fault (Figure 1b) provides the access for groundwater flow as manifested by the widespread distribution of hot springs (Jiang et al., 2016). The surface of the valley is blanketed by Holocene-aged colluvium, filled with the great thickness of alluvial-pluvial sediments from the south such as gravel, sandy loam, and clay. The vegetation in the catchment is characterized by alpine meadow, alpine steppe, marsh, shrub, etc, and meadow and marsh are mainly distributed in the valley and river source (Zhang et al., 2010).

Located on the south-central TP, the Yangbajain Catchment is a glacier-fed headwater catchment with significant frozen ground coverage (Figures 1b & 1c). A majority of glaciers were found along the Nyainqêntanglha Ranges (Figure 1b). Glaciers cover over ten percent of the whole catchment, making it the most glacierized sub-basin in the Lhasa River Basin. According to the First Chinese Glacier Inventory (Mi et al., 2002), the total glacier area was about 316.31 km^2 in 1960. The ablation period of the glaciers ranges from June to September with the glacier termini

145 at about 5,200 m (Liu et al., 2011). According to the new map of permafrost
146 distribution on the TP (Zou et al., 2017), the valley is underlain by seasonally frozen
147 ground (Figure 1c). It is estimated that seasonally frozen ground and permafrost
148 accounts for about 64% and 36% of the total catchment area, respectively (Zou et al.,
149 2017). The lower limit of alpine permafrost is around 4,800 m, and the thickness of
150 permafrost varies from 5 m to 100 m (Zhou et al., 2000).

151 The catchment is characterized by a semi-arid temperate monsoon climate. The
152 areal average annual air temperature of the Yangbajain Catchment is approximately
153 -2.3°C with monthly variation from -8.6°C in January to 3.1°C in July (Figure 2). The
154 average annual precipitation at the Yangbajain Station is about 427 mm. The
155 catchment has a summer (June-August) monsoon with 73% of the yearly precipitation,
156 while the rest of the year is dry with only 1% of the yearly precipitation occurring in
157 winter (December-February) (Figure 2).

158 The average annual streamflow at the Yangbajain Station is 277.7 mm, and the
159 intra-annual distribution of streamflow is uneven (Figure 2). In summer, streamflow is
160 recharged mainly by monsoon rainfall and meltwater, and the volume of summer
161 runoff accounts for approximately 63% of the yearly streamflow (Figure 2). The
162 streamflow in winter with only 4% of the yearly streamflow (Figure 2) is only
163 recharged by groundwater, which is greatly affected by the freeze-thawing cycle of
164 frozen ground and the active layer (Liu et al., 2011).

165 **2.2. Data**

166 Daily streamflow and precipitation data at four hydrological Stations (Figure 1a)
167 during the period 1979-2013 are adopted for assessing the changes of stream flow in a
168 warming climate. The monthly meteorological data at three weather stations (Figure
169 1a) are obtained from the China Meteorological Data Sharing Service System
170 (http://data.cma.cn/) for the years from 1979 to 2013. In this study, the method of
171 meteorological data extrapolation by Prasch et al. (2013) is adopted to obtain the
172 discretisized air temperature (with cell size as 1 km×1 km) of the Lhasa River Basin
173 based on the air temperature of the three stations assuming a linear lapse rate. The
174 mean monthly lapse rate is set to 0.44 °C/100 m for elevations below 4,965 m and
175 0.78 °C/100 m for elevations above 4,965 m in the catchment (Wang et al., 2015).
176 The glaciers and frozen ground data are provided by the Cold and Arid Regions
177 Science Data Center (http://westdc.westgis.ac.cn/). The distribution, area and volume
178 of glaciers are based on the First and Second Chinese Glacier Inventory in 1960 and
179 2009 (Mi et al., 2002; Liu et al., 2014) (Figure 1b). The distribution and classification
180 of frozen ground (Figure 1c) are collected from the twice maps of frozen ground on
181 the TP (Li and Cheng, 1996; Zou et al., 2017).
182 The latest Level-3 monthly mascon solutions (CSR, Save et al., 2016) was used to
183 detect terrestrial water storage (TWS, total vertically-integrated water storage)
184 changes for the period from January 2003 to December 2015 with spatial sampling of
185 0.5°×0.5° from the Gravity Recovery and Climate Experiment (GRACE) satellite.
186 The time series of 2003~2015 for snow water equivalent (SWE), total soil moisture

(SM, layer 0~200cm) from the dataset (GLDAS_Noah2.1, https://disc.gsfc.nasa.gov/) were adopted for derivation of the groundwater storage (GWS) (Richey et al., 2015).

2.3. Methods

2.3.1. Statistical methods for assessing streamflow changes

The Mann-Kendall (MK) test, which is suitable for data with non-normally distributed or nonlinear trends, is applied to detect trends of hydro-meteorological time series (Mann, 1945; Kendall, 1975). To remove the serial correlation from the examined time series, a Trend-Free Pre-Whitening (TFPW) procedure is needed prior to applying the MK test (Yue et al., 2002). A more detailed description of the Trend-Free Pre-Whitening (TFPW) approach was provided by Yue et al. (2002).

Gray relational analysis was aimed to find the major climatic or hydrological factors that influenced an objective variable (Liu et al., 2005; Wang et al., 2013). In this paper, gray relational analysis is used to investigate the main climatic factors impacting the streamflow changes.

2.3.2. Baseflow separation

In this paper, the most widely used one-parameter digital filtering algorithm is adopted for baseflow separation (Lyne and Hollick, 1979). The filter equation is expressed as

$$q_t = \alpha q_{t-1} + \frac{1+\alpha}{2}\left(Q_t - Q_{t-1}\right) \quad (1)$$

$$b_t = Q_t - q_t \quad (2)$$

where q_t and q_{t-1} are the filtered quick flow at time step t and t-1, respectively; Q_t and

208 Q_{t-1} are the total runoff at time step t and t-1; α is the filter parameter that ranging
209 from 0.9 to 0.95; b_t is the filtered baseflow.

210 *2.3.3. Determination of active groundwater storage*

211 In this study, the active groundwater storage (abbreviated as groundwater storage in
212 the following context) is assumed as a storage that directly controls streamflow
213 dynamics during rainless periods (Kirchner, 2009; Staudinger, 2017). Based on
214 hydraulic groundwater theory, groundwater storage in a catchment can be
215 approximated as a power function of baseflow rate at the catchment outlet (Brutsaert,
216 2008).

217 $$S = Ky^m \tag{8}$$

218 where y is the rate of baseflow in the stream, and S is the volume of active
219 groundwater storage in the catchment aquifers under climate warming (see in Figure
220 3). Here K, m are constants depending on the catchment physical characteristics, and
221 K is the baseflow recession coefficient, which represents the time scale of the
222 catchment streamflow recession process.

223 During dry season without precipitation and other input events, the conservation of
224 mass equation can be represented as

225 $$\frac{dS}{dt} = -y \tag{9}$$

226 where t is the time. Substitution of equation (8) in equation (9) yields (Brutsaert and
227 Nieber, 1977)

$$-\frac{dy}{dt} = ay^b \tag{10}$$

where dy/dt is the temporal change of the baseflow rate during recessions, and the constants a and b are called the recession intercept and recession slope of plots of $-dy/dt$ versus y in log-log space, respectively. In the storage discharge relationship, the aquifer responds as a linear reservoir if b=1, and as nonlinear reservoir if b≠1. In addition, with a fixed slope b, the changes in catchment aquifer properties by fitting the intercept a as a variable can be observed (Rupp and Selker, 2006).

According to Gao et al. (2017), the parameters of K and m in equation (8) can be expressed by a and b, where $K = 1/\left[a\left(2-b\right)\right]$ and $m = 2-b$. Furthermore, the constants a and b can be determined through the technique of recession slope curves. In this study, the two constants are curve-fitted by using a nonlinear least squares regression through all data points of $-dy/dt$ versus y in log-log space for all years to avoid the difficulty of defining a lower envelop of the scattered points (Lyon et al., 2009). According to the values of a and b, K and m can be calculated. Thus the average groundwater storage S for dry season can be obtained through equation (8) based on average rate of baseflow.

3. Results

3.1. Assessment of streamflow changes

The annual streamflow of the Yangbajain Catchment shows an increasing trend at the 5% significance level with a mean rate of about 12.30 mm/10a over the period 1979-2013 (Table 1 and Figure 4a). Meanwhile, annual mean air temperature exhibits

249 an increasing trend at the 1% significance level with a mean rate of about 0.28 °C/10a
250 (Table 1 and Figure 5a). However, annual precipitation has a nonsignificant trend
251 during this period (Table 1 and Figure 5b).

252 As annual streamflow increases significantly, it is necessary to analyze to what
253 extent the changes in the two components (quick flow and baseflow) lead to
254 streamflow increases. Based on the baseflow separation method, the annual mean
255 baseflow contributes about 59% of the annual mean streamflow in the catchment. The
256 MK test shows that annual baseflow exhibits a significant increasing trend at the 1%
257 level with a mean rate of about 10.95 mm/10a over the period 1979-2013 (Table 1 and
258 Figure 4b). But the trend is statistically nonsignificant for annual quick flow in the
259 same period (Table 1). The increasing trends between the baseflow and streamflow
260 are very close, indicating that the increase in baseflow is the main contributor to
261 streamflow increases.

262 Furthermore, gray relational analysis is applied to the catchment to identify the
263 major climatic factors for the increasing streamflow. The result shows that the air
264 temperature has a higher gray relational grade at annual scale (Table 2). This indicates
265 that the air temperature acts as a primary factor for the increased streamflow as well
266 as the baseflow.

267 The annual streamflow and baseflow significantly increase due to the rising air
268 temperature over the period 1979-2013. However, there are diverse intra-annual
269 variation characteristics for streamflow as well as the two streamflow components

during the period. Streamflow in spring (March to May), autumn (September to November) and winter (December to February) show increasing trends at least at the 5% significance level (Figure 6a, 6c and 6d), while streamflow in summer (June to August) has a nonsignificant trend during this period (Figure 6b). Baseflow also increases significantly in spring, autumn and winter (Figure 6a, 6c and 6d). The trend is statistically nonsignificant for baseflow in summer (Figure 6b). Quick flow exhibits nonsignificant trend for all seasons (Table 1). As to the meteorological factors, mean air temperature in all seasons increase significantly at the 1% level especially during winter with the rate of about 0.51°C/10a (Table 1 and Figure 7), whereas precipitation in each season shows nonsignificant trend during these years (Table 1). The gray relational analysis shows that the air temperature is a critical climatic factor for the changes in streamflow and baseflow in all seasons (Table 2).

3.2. Estimation of groundwater storage by baseflow recession analysis

Daily streamflow and precipitation records in autumn and early winter (September to December) was adopted. In this dry season, hydrograph usually with little precipitation declines consecutively and smoothly. The fitted slope b is equal to 1.79 through the nonlinear least square fit of equation (10) for all data points of $-dy/dt$ versus y in log-log space during the period 1979-2013. Moreover, for each decade or year, the intercept a could be fitted by the fixed slope b=1.79. Then, the values of K and m for each decade or year can be determined. And the groundwater storage S for each year can be directly estimated from the average rate of baseflow during a

recession period through equation (8).

Figure 8 shows the results of the nonlinear least square fit for each decade's recession data from the 1980s, 1990s and 2000s, respectively. As shown in Figure 8, the recession data points and fitted recession curves of each decade gradually move downward as time goes on. This indicates that, with a fixed slope *b*, the intercept *a* gradually decreases and recession coefficient *K* increases accordingly. The values of recession coefficient *K* for each decade are 77 $mm^{0.79}d^{0.21}$, 84 $mm^{0.79}d^{0.21}$ and 103 $mm^{0.79}d^{0.21}$. Furthermore, Figure 9a shows the inter-annual variation of recession coefficient *K* during the period 1979-2013. In total, though there are some large fluctuations or even a rather large decrease at the beginning of the 1990s, the overall increasing trend of 7.70 $(mm^{0.79}d^{0.21})$/10a at a significance level of 5% is similar to the results obtained from decade analysis. This long-term variation of recession coefficient *K* from September to December indicates that baseflow recession during autumn and early winter gradually slows down in the catchment.

According to the results of decade data fit (see in Figure 8), the mean values of groundwater storage *S* estimated for each decade are 130 mm, 148 mm and 188 mm for the 1980s, 1990s and 2000s. The inter-annual variation of groundwater storage *S* is also similar with recession coefficient *K* (Figure 9a and 9b). The decreased trend of anomalies changes of groundwater storage (*GWS*) estimated by the GRACE data is consistent with the annual trend of *S* during 2003~2015 (Figure 9b). And the reduced volume of groundwater between *GWS* and *S* are also comparable (~100-120 mm),

312 which has partly verified our estimations.

313 The trend analysis suggests that the groundwater storage *S* shows an increasing
314 trend at the 5% significance level with a rate of about 19.32 mm/10a during the period
315 1979-2013 (Figure 9b). The annual trend of groundwater storage *S* from 1979 to 2013
316 is consistent with the values across decades. This indicates that groundwater storage
317 has been enlarged. Through recent field investigations, we know that groundwater
318 level is rising. The increases of surface water and shallow groundwater storages are
319 changing the land cover. For example, the Normalized Difference Vegetation Index
320 (NDVI) is rising accordingly in the past twenty years (Figure 10). In fact, not only in
321 the study area but also in the whole TP, surface water and groundwater storage are
322 increasing due to climate warming, and hence vegetation conditions have been
323 improved (Zhang et al., 2018; Khadka et al., 2018).

324 **4. Discussions**

325 The results have revealed that the increase of streamflow especially in dry season is
326 tightly related with climate warming. It is obviously that both glacier retreat and
327 frozen ground degradation in a warmer climate can significantly alter the mechanism
328 of streamflow. In the Yangbajain Catchment as well as the whole Lhasa River Basin,
329 it is experiencing a noticeable glacier retreat and frozen ground degradation during the
330 past decades (Table 3). For instance, according to the twice map of frozen ground
331 distribution on the TP (Li and Cheng, 1996; Zou et al., 2017), the areal extent of
332 permafrost in the Yangbajain catchment has decreased by 406 km^2 (15.3%) over the

past 22 years; the areal extent of seasonal frozen ground has increased by 406 km^2 (15.3%) with the corresponding degradation of permafrost.

According to the new map of permafrost distribution on the Tibetan Plateau (Zou et al., 2017), the coverages of permafrost and seasonally frozen ground in each sub-catchment (especially the Lhasa sub-catchments) are comparable to that in the Yangbajain Catchment; but the coverage of glaciers in the three catchments is far lower than that in the Yangbajain Catchment according to the First Chinese Glacier Inventory (Mi et al., 2002) (Table 3). The MK test showed that, in all the four catchments, the annual mean air temperature had significant increases at the 1% significance level while the annual precipitation showed nonsignificant trends (Table 4). The changes of annual streamflow of the Lhasa, Pangdo and Tangga Catchments had nonsignificant trends. The reason is that compared with the Yangbajain Catchment all the three larger sub-catchments as well as the whole Lhasa River Basin possess relatively smaller glacier coverage, in which summer rainfall contributes 48% of the total runoff according to Guan et al. (1984). While the annual streamflow of the Yangbajain Catchment showed an increasing trend at the 5% significance level with a mean rate of about 12.30 mm/10a during the period. Ye et al. (1999) stated that when glacier coverage is greater than 5%, glacier contribution to streamflow induced by climate warming starts to show up. As reported by Prasch et al. (2013), the contribution of accelerated glacial meltwater to streamflow would bring a significant increase in streamflow in the Yangbajain Catchment. Thus it is reasonable to attribute

annual streamflow increases to the accelerated glacier retreat as the consequence of increasing annual air temperature in the Yangbajain Catchment.

Although permafrost degradation is not the controlling factor for the increase of streamflow, a rational hypothesis is that increased groundwater storage *S* in autumn and early winter is associated with frozen ground degradation, which can enlarge groundwater storage capacity (Niu et al., 2016). Figure 3 depicts the changes of surface flow and groundwater flow paths in a glacier fed catchment, which is underlain by frozen ground under past climate and warmer climate, respectively. As frozen ground extent continues to decline and active layer thickness continues to increase in the valley, the enlargement of groundwater storage capacity can provide enough storage space to accommodate the increasing meltwater that may percolate into deeper aquifers (Figure 3). Then, the increase of groundwater storage in autumn and early winter allows more groundwater discharge into streams as baseflow, and lengthens the recession time as indicated by the recession coefficient *K*. This leads to the increased baseflow and slow baseflow recession in autumn and early winter, as is shown in Figure 6c, 6d and Figure 9a. In the late winter and spring, the increase of baseflow (Figure 6d and 6a) can be explained by the delayed release of increased groundwater storage.

Thus, as the results of climate warming, river regime in this catchment has been altered significantly. On the one hand, permafrost degradation is changing the aquifer structure that controls the storage-discharge mechanism, e.g., catchment groundwater

storage increases at about 19.32 mm/10a. On the other hand, huge amount of water from glacier retreat is contributing to the increase of streamflow and groundwater storage. For example, the annual streamflow of the Yangbajain Catchment increases with a mean rate of about 12.30 mm/10a during the past 50 years. However, the total glacial area and volume have decreased by 38.05 km^2 (12.0%) and 1788 mm (26.2%) over the period 1960-2009 (Figure 11) according to the Chinese Glacier Inventories. Hence, the reduction rate of glacial volume is 9.46×10^7 m^3/a (about 357.7 mm/10a) on average during the past 50 years. In the ablation on continental type glaciers in China, evaporation (sublimation) always takes an important role, however, annul amount of evaporation is usually less than 30% of the total ablation of glaciers in the high mountains of China (Zhang et al., 1996). Given the 30% reduction in glacial melt, there is still a large water imbalance between the melt-derived runoff and the actually increase of runoff and groundwater storage. Our results imply that more than 60% of glacial meltwater would be lost by subsurface leakage.

5. Conclusions

In this study, the changes of hydro-meteorological variables were evaluated to identify the main climatic factor for streamflow changes in the cryospheric Yangbajain Catchment. We find that the annual streamflow especially the annual baseflow increases significantly, and the rising air temperature acts as a primary factor for the increased runoff. Furthermore, through parallel comparisons of sub-basins in the Lhasa River Basin, we presumed that the increased streamflow in the Yangbajain

catchment is mainly fed by glacier retreat. Due to the climate warming, the total glacial area and volume have decreased by 38.05 km^2 (12.0%) and 4.73×10^9 m^3 (26.2%) in 1960-2009, and the areal extent of permafrost has degraded by 406 km^2 (15.3%) in the past 22 years. As a results of permafrost degradation, groundwater storage capacity has been enlarged, which triggers a continuous increase of groundwater storage at a rate of about 19.32 mm/10a. This can explain why baseflow volume increases and baseflow recession slows down in autumn and early winter.

At last we find that there is a large water imbalance (> 5.79×10^7 m^3/a) between the melt-derived runoff and the actually increase of runoff and groundwater storage, which suggests more than 60% of the reduction in glacial melt should be lost by subsurface leakage. However, the pathway of these leakage is still an open question for further studies. More methods (e.g., hydrological isotopes) should be adopted to quantify the contribution of glaciers meltwater and permafrost degradation to streamflow, and to explore the change of groundwater storage capacity as frozen ground continues to degrade.

Code/Data availability

The code and data used in this study are available from the authors on request.

Author contributions.

LL and JL provided insights; LL and MG performed the coding and analysis; LL drafted the paper with contributions from all the co-authors. JL and XC collected the data. JL, JW, SW and HL contributed to analysis of the results, the discussion and

417 manuscript editing.

418 **Competing interests.**

419 The authors declare that they have no conflict of interest.

420 **Acknowledgements**

421 We would like to thank editor Fuqiang Tian, Dr. Van Hoy and the other anonymous
422 reviewers, whose perceptive criticisms, comments and suggestions helped us improve
423 the quality of the manuscript.

424 **Financial support.**

425 This work was supported by the Second Tibetan Plateau Scientific Expedition and
426 Research Program (STEP) (2019QZKK0207), the National Natural Science
427 Foundation of China (NSFC) (91647108, 91747203), the West Light Foundation of
428 the Chinese Academy of Sciences (29Y929621) and the Special Fund of the State Key
429 Laboratory of Hydrology-Water Resources and Hydraulic Engineering
430 (20185044312).

431 **References**

432 Bense, V. F., Kooi, H., Ferguson, G., and Read, T.: Permafrost degradation as a
433 control on hydrogeological regime shifts in a warming climate, Journal of
434 Geophysical Research Earth Surface, 117, F03036, doi:10.1029/2011JF002143,
435 2012.
436 Bibi, S., Wang, L., Li, X. P., Zhou, J., Chen, D. L., and Yao, T. D.: Climatic and
437 associated cryospheric, biospheric, and hydrological changes on the Tibetan Plateau:
438 A review, International Journal of Climatology, 38, e1-e17, doi:10.1002/joc.5411,

2018.

Brutsaert, W., and Nieber, J. L.: Regionalized drought flow hydrographs from a mature glaciated plateau, Water Resources Research, 13(3), 637-643, 1977.

Brutsaert, W.: Long-term groundwater storage trends estimated from streamflow records: Climatic perspective, Water Resources Research, 44(2), 114-125, doi:10.1029/2007WR006518, 2008.

Buttle, J. M.: Mediating stream baseflow response to climate change: the role of basin storage, Hydrological Processes, 32(1), doi:10.1002/hyp.11418, 2017.

Chapman, T.: A comparison of algorithms for stream flow recession and baseflow separation, Hydrological Processes, 13, 701-714, 1999.

Cheng, G. D., and Wu, T. H.: Responses of permafrost to climate change and their environmental significance, Qinghai-Tibet Plateau, Journal of Geophysical Research Earth Surface, 112, F02S03, doi:10.1029/2006JF000631, 2007.

Cuo, L., Zhang, Y. X., Zhu, F. X., and Liang, L. Q.: Characteristics and changes of streamflow on the Tibetan Plateau: A review, Journal of Hydrology Regional Studies, 2, 49-68, doi:10.1016/j.ejrh.2014.08.004, 2014.

Duan, L., Man, X., Kurylyk, B.L., Cai, T.: Increasing winter baseflow in response to permafrost thaw and precipitation regime shifts in northeastern China, Water, 9, 25, doi:10.3390/w9010025, 2017.

Gao, M., Chen, X., Liu, J., Zhang, Z., and Cheng, Q.: Using two parallel linear reservoirs to express multiple relations of power-law recession curves, Journal of Hydrologic Engineering, 04017013, doi:10.1061/(ASCE)HE.1943-5584.0001518, 2017.

Ge, S., J. McKenzie, C. Voss, and Wu, Q.: Exchange of groundwater and surface-water mediated by permafrost response to seasonal and long term air temperature variation, Geophysical Research Letters, 38, L14402, doi:10.1029/2011GL047911, 2011.

Guan, Z. H., Chen, C. Y., Kuang, Y. X., Fan Y. Q., Zhang, Y. S., and Chen, Z. M. et al.: Rivers and Lakes in Tibetan. Rivers and lakes in Tibet. Beijing: Science and Technology Press, 1984 (in Chinese).

Green, T. R., Taniguchi, M., Kooi, H., Gurdak, J. J., Allen, D. M., and Hiscock, K. M., et al.: Beneath the surface of global change: impacts of climate change on groundwater, Journal of Hydrology, 405(3), 532-560, doi:10.1016/j.jhydrol.2011.05.002, 2011.

Immerzeel, W. W., van Beek, L. P. H., and Bierkens, M. F. P.: Climate change will affect the Asian water towers, Science, 328, 1382-1385, 2010.

Jiang, W., Han, Z., Zhang, J., and Jiao, Q.: Stream profile analysis, tectonic geomorphology and neotectonic activity of the Damxung-Yangbajain Rift in the south Tibetan Plateau, Earth Surface Processes and Landforms, 41(10), 1312-1326, doi:10.1002/esp.3899, 2016.

Kang, S. C., Xu, Y. W., You, Q. L., Flügel, W. A., Pepin, N., and Yao, T. D.: Review of climate and cryospheric change in the Tibetan Plateau, Environmental Research Letters, 5(1), 015101, doi:10.1088/1748-9326/5/1/015101, 2010.

Käser, D., and D. Hunkeler.: Contribution of alluvial groundwater to the outflow of mountainous catchments, Water Resources Research, 52, 680-697, doi:10.1002/2014WR016730, 2016.

Kendall, M. G.: Rank Correlation Methods, 4th ed, Charles Griffin, London, pp. 196, 1975.

Khadka, N., Zhang, G., and Thakuri, S.: Glacial Lakes in the Nepal Himalaya: Inventory and Decadal Dynamics (1977–2017). Remote Sensing, 10, 1913, doi:10.3390/rs10121913, 2018.

Kooi, H., Ferguson, G., Bense, V. F.: Evolution of shallow groundwater flow systems in areas of degrading permafrost, Geophysical Research Letters, 36(22):297-304, 2009.

493 Kirchner, J.W.: Catchments as simple dynamical systems: catchment characterization,
494 rainfall-runoff modeling, and doing hydrology backward, Water Resources
495 Research, 45, W02429, doi:10.1029/2008WR006912, 2009.
496 Li, S., and Cheng, G.: Map of Frozen Ground on Qinghai-Xizang Plateau, Gansu
497 Culture Press, Lanzhou, 1996.
498 Li, Z. J., Li, Z. X., Song, L. L., Ma, J. Z., and Song Y.: Environment significance and
499 hydrochemical characteristics of suprapermafrost water in the source region of the
500 Yangtze River, Science of the Total Environment, 644, 1141-1151, 2018.
501 Lin, K. T., and Yeh, H. F.: Baseflow recession characterization and groundwater
502 storage trends in northern Taiwan, Hydrology Research, 48(6), 1745-1756, 2017.
503 Liu, J. S., Xie, J., Gong, T. L., Wang, D., and Xie, Y. H.: Impacts of winter warming
504 and permafrost degradation on water variability, upper Lhasa River, Tibet,
505 Quaternary International, 244(2), 178-184, doi:10.1016/j.quaint.2010.12.018, 2011.
506 Liu, J. T., Han, X. L., Chen, X., Lin, H., and Wang, A. H.: How well can the
507 subsurface storage-discharge relation be interpreted and predicted using the
508 geometric factors in headwater areas? Hydrological Processes, 30(25), 4826-4840,
509 doi:10.1002/hyp.10958, 2016.
510 Liu, Q. Q, Singh, V. P., and Xiang, H.: Plot erosion model using gray relational
511 analysis method, Journal of Hydrologic Engineering, 10, 288-294, 2005.
512 Liu, S. Y., Guo, W., and Xu, J., et al.: The Second Glacier Inventory Dataset of China
513 (Version 1.0), Cold and Arid Regions Science Data Center at Lanzhou, 2014,
514 doi:10.3972/glacier.001.2013.db.
515 Liu, X. D., and Chen, B. D.: Climatic warming in the Tibetan Plateau during recent
516 decades, International Journal of Climatology, 20(14), 1729-1742, 2000.
517 Lyne, V., and Hollick, M.: Stochastic time-variable rainfall-runoff modeling, Aust.
518 Natl. Conf. Publ. pp.89-93, 1979.
519 Lyon, S. W., and Destouni, G.: Changes in catchment-scale recession flow properties

520 in response to permafrost thawing in the Yukon River basin, International Journal
521 of Climatology, 30(14), 2138-2145, doi:10.1002/joc.1993, 2010.
522 Lyon, S. W., Destouni, G., Giesler, R., Humborg, C., Mörth, M., and Seibert, J., et al.:
523 Estimation of permafrost thawing rates in a sub-arctic catchment using recession
524 flow analysis, Hydrology and Earth System Sciences, 13(5), 595-604, 2009.
525 Mann, H.: Non-parametric test against trend, Econometrica, 13, 245-259, 1945.
526 Mi, D. S., Xie, Z. C., and Luo, X. R.: Glacier Inventory of China (volume XI: Ganga
527 River drainage basin and volume XII: Indus River drainage basin). Xi'an
528 Cartographic Publishing House, Xi'an, pp. 292-317, 2002 (In Chinese).
529 Niu, L., Ye, B. S., Li, J., and Sheng, Y.: Effect of permafrost degradation on
530 hydrological processes in typical basins with various permafrost coverage in
531 western China, Science China Earth Sciences, 54(4), 615-624,
532 doi:10.1007/s11430-010-4073-1, 2011.
533 Niu, L., Ye, B., Ding, Y., Li, J., Zhang, Y., Sheng, Y., and Yue, G.: Response of
534 hydrological processes to permafrost degradation from 1980 to 2009 in the upper
535 Yellow River basin, China, Hydrology Research, 47(5), 1014-1024,
536 doi:10.2166/nh.2016.096, 2016.
537 Patnaik, S., Biswal1, B., Kumar, D. N., Sivakumar, B.: Regional variation of
538 recession flow power-law exponent, Hydrological Processes, 32, 866–872, 2018.
539 Prasch, M., Mauser, W., and Weber, M.: Quantifying present and future glacier
540 melt-water contribution to runoff in a central Himalayan river basin, Cryosphere,
541 7(3), 889-904, doi:10.5194/tc-7-889-2013, 2013.
542 Pritchard, H. D.: Asia's glaciers are a regionally important buffer against drought,
543 Nature, 545(7653), 169, doi:10.1038/nature22062, 2017.
544 Richey, A. S., Thomas, B. F., Lo, M.-H., Reager, J. T., Famiglietti, J. S., Voss, K.,
545 Swenson, S., and Rodell, M.: Quantifying renewable groundwater stress with
546 GRACE, Water Resources Research, 51, 5217–5238, doi:10.1002/ 2015WR017349,

2015.

Rogger, M., Chirico, G. B., Hausmann, H. Krainer, K. Brückl, E. Stadler, P. and Blöschl, G.: Impact of mountain permafrost on flow path and runoff response in a high alpine catchment, Water Resources Research, 53, 1288-1308, doi:10.1002/2016WR019341, 2017.

Rupp, D. E., and Selker, J. S.: Information, artifacts, and noise in d*Q*/d*t*-*Q* recession analysis, Advances in Water Resources, 29(2), 154-160, 2006.

Save, H., Bettadpur, S., and Tapley, B. D.: High-resolution CSR GRACE RL05 masons, Journal of Geophysical Research: Solid Earth, 121, 7547–7569, doi.org/10.1002/2016JB013007, 2016.

Staudinger, M., Stoelzle, M., Seeger, S., Seibert, J., Weiler, M., and Stahl, K.: Catchment water storage variation with elevation, Hydrological Processes, 31(11), doi:10.1002/hyp.11158, 2017.

Su, F., Zhang, L., Ou, T., Chen, D., Yao, T., Tong, K., and Qi, Y.: Hydrological response to future climate changes for the major upstream river basins in the Tibetan Plateau. Global and Planetary Change, 136, 82-95, doi:10.1016/j.gloplacha.2015.10.012, 2016.

Viviroli, D., Du¨rr, H. H., Messerli, B., Meybeck, M., and Weingartner, R.: Mountains of the world, water towers for humanity: Typology, mapping, and global significance, Water Resources Research, 43, W07447, doi:10.1029/2006WR005653, 2007.

Walvoord, M. A., and Kurylyk, B. L.: Hydrologic impacts of thawing permafrost-A review, Vadose Zone Journal, 15(6), doi:10.2136/vzj2016.01.0010, 2016.

Walvoord, M. A., and Striegl, R. G.: Increased groundwater to stream discharge from permafrost thawing in the Yukon River basin: Potential impacts on lateral export of carbon and nitrogen, Geophysical Research Letters, 34(12), 123-134, doi:10.1029/2007GL030216, 2007.

574 Wang, G., Mao, T., Chang, J., Song, C., and Huang, K.: Processes of runoff
575 generation operating during the spring and autumn seasons in a permafrost
576 catchment on semi-arid plateaus, Journal of Hydrology, 550, 307-317, 2017.
577 Wang, S., Liu, S. X., Mo, X. G., Peng, B., Qiu, J. X., Li, M. X., Liu, C. M., Wang, Z.
578 G., and Bauer-Gottwein, P.: Evaluation of remotely sensed precipitation and its
579 performance for streamflow simulations in basins of the southeast Tibetan Plateau,
580 Journal of Hydrometeorology, 16(6), 342-354, doi:10.1175/JHM-D-14-0166.1,
581 2015.
582 Wang, W. F., Wu, T. H., Zhao, L., Li R., Zhu X. F., Wang, W. R., Yang, S. H., Qin, Y.
583 H., and Hao, J. M.: Exploring the ground ice recharge near permafrost table on the
584 central Qinghai-Tibet Plateau using chemical and isotopic data, Journal of
585 Hydrology, 560, 220-229, 2018.
586 Wang, Y. F., Shen, Y. J., Chen, Y. N., and Guo, Y.: Vegetation dynamics and their
587 response to hydroclimatic factors in the Tarim River Basin, China, Ecohydrology,
588 6(6), 927-936, 2013.
589 Wang, Y. H., Yang, H. B., Gao, B., Wang, T. H., Qin, Y., and Yang, D. W.: Frozen
590 ground degradation may reduce future runoff in the headwaters of an inland river
591 on the northeastern Tibetan Plateau, Journal of Hydrology, 564, 1153-1164, 2018.
592 Wittenberg, H.: Baseflow recession and recharge as nonlinear storage processes,
593 Hydrological Processes, 13, 715-726, 1999.
594 Woo, M. K., Kane, D. L., Carey, S. K., and Yang, D.: Progress in permafrost
595 hydrology in the new millennium, Permafrost & Periglacial Processes, 19(2),
596 237-254, doi:10.1002/ppp.613, 2008.
597 Wu, Q. B., and Zhang, T. J.: Recent permafrost warming on the Qinghai-Tibetan
598 Plateau, Journal of Geophysical Research Atmospheres, 113, D13108,
599 doi:10.1029/2007JD009539, 2008.
600 Wu, Z. H., and Zhao, X. T.: Quaternary geology and faulting in the

601 Damxung-Yangbajain Basin, southern Tibet, Journal of Geomechanics, 12(3),
602 305-316, 2006 (in Chinese).
603 Xu, M., Kang, S., Wang, X., Pepin, N., and Wu H.: Understanding changes in the
604 water budget driven by climate change in cryospheric-dominated watershed of the
605 northeast Tibetan Plateau, China, Hydrological Processes, 1-19, doi:10.1002/hyp.
606 13383, 2019.
607 Yang, G., Lei, D., Hu, Q., Cai, Y., and Wu, J.: Cumulative coulomb stress changes in
608 the basin-range region of Gulu-Damxung-Yangbajain and their effects on strong
609 earthquakes, Electronic Journal of Geotechnical Engineering, 22(5), 1523-1530,
610 2017.
611 Yao, T. D., Pu, J. C., Lu, A. X., Wang, Y. Q., and Yu, W. S.: Recent glacial retreat and
612 its impact on hydrological processes on the Tibetan Plateau, China, and
613 surrounding regions, Arctic, Antarctic, and Alpine Research, 39(4), 642-650, 2007.
614 Yao, T. D., Wang, Y. Q., Liu, S. Y., Pu, J. C., Shen, Y. P., and Lu, A. X.: Recent glacial
615 retreat in high Asia in China and its impact on water resource in northwest China,
616 Science in China, 47(12), 1065-1075, doi:10.1360/03yd0256, 2004.
617 Ye, B. S., Han, T. D., Ding, Y. J.: Some Changing Characteristics of Glacier
618 Streamflow in Northwest China, Journal of Glaciolgy and Geocryology,
619 21(1):54-58, 1999 (in Chinese).
620 Yue, S., Pilon, P., Phinney, B., and Cavadias, G.: The influence of autocorrelation on
621 the ability to detect trend in hydrological series, Hydrological Processes, 16(9),
622 1807-1829, doi:10.1002/hyp.1095, 2002.
623 Zhang, Y., Yao, T. D., and Pu, J. C.: The characteristics of ablation on continental-type
624 glaciers in China, Journal of Glaciology and Geocryology, 18(2), 147-154, 1996 (in
625 Chinese).
626 Zhang, Y., Wang, C., and Bai, W., et al.: Alpine wetland in the Lhasa River Basin,
627 China, Journal of Geographical Sciences, 20(3): 375-388, 2010 (in Chinese).

628 Zhang, Z. X., Chang, J., and Xu, C. Y., et al.: The response of lake area and vegetation
629 cover variations to climate change over the Qinghai-Tibetan Plateau during the past
630 30 years, Science of the Total Environment, 635, 443-451, 2018.
631 Zhou, Y. W., Guo, D. X., Qiu, G. Q., Cheng, G. D., and Li, S. D.: Permafrost in China,
632 Science Press, Beijing, pp. 63-70, 2000 (In Chinese).
633 Zou, D., Zhao, L., Sheng, Y., and Chen, J., et al.: A new map of permafrost
634 distribution on the Tibetan Plateau, The Cryosphere, 11, 2527-2542,
635 doi:10.5194/tc-11-2527-2017, 2017.
636

637

Table 1. Mann-Kendall trend test with trend-free pre-whitening of seasonal and annual mean air temperature (°C), precipitation (mm), streamflow (mm), baseflow (mm) and quick flow (mm) from 1979 to 2013.

	Air temperature		Precipitation		Streamflow		Baseflow		Quick flow	
	Z_C	β (°C/a)	Z_C	β (mm/a)	Z_C	β (mm/a)	Z_C	β (mm/a)	Z_C	β (mm/a)
Spring	2.73**	0.026	0.90	0.290	3.05**	0.206	2.99**	0.147	0.98	0.042
Summer	2.63**	0.013	1.30	2.139	0.92	0.549	1.27	0.429	0.50	0.128
Autumn	2.65**	0.024	-0.68	-0.395	2.46*	0.546	2.96**	0.476	0.80	0.074
Winter	3.49**	0.051	-0.46	-0.014	3.08**	0.204	2.13*	0.145	1.39	0.016
Annual	4.48**	0.028	1.28	2.541	2.07*	1.230	2.70**	1.095	0.77	0.327

Comment: the symbols of Z_C and β mean the standardized test statistic and the trend magnitude, respectively; positive values of Z_C and β indicate the upward trend, whereas negative values indicate the downward trend in the tested time series; the symbols of asterisks *and ** mean statistically significant at the levels of 5% and 1%, respectively.

Table 2. Gray relational grades between the streamflow/baseflow and climate factors (precipitation and air temperature) in the Yangbajain Catchment at both annual and seasonal scales. Bold text shows the higher gray relational grade in each season.

	G_{oi} with the streamflow		G_{oi} with the baseflow	
	Precipitation	Air temperature	Precipitation	Air temperature
Spring	0.690	**0.778**	0.713	**0.789**
Summer	0.689	**0.784**	0.680	**0.776**
Autumn	0.653	**0.667**	0.648	**0.680**
Winter	0.742	**0.886**	0.748	**0.895**
Annual	0.675	**0.727**	0.665	**0.729**

638 Comment: G_{oi} is the gray relational grade between the streamflow/baseflow and climate factors. The importance of each influence factor can be determined by the
639 order of the gray relational grade values. The influence factor with the largest G_{oi} is regarded as the main stress factor for the objective variable.

640 **Table 3.** The coverage of glaciers and frozen ground in four catchments of the Lhasa River Basin

Stations	Area (km^2)	Glaciers(1960)		Glaciers(2009)		Permafrost (1996)		Permafrost (2017)		Seasonally frozen ground (1996)		Seasonally frozen ground (2017)	
		Area (km^2)	Coverage (%)	Area (km^2)	Coverage (%)	Area (km^2)	Coverage (%)	Area (km^2)	Coverage (%)	Area (km^2)	Coverage (%)	Area (km^2)	Coverage (%)
Lhasa	26233	349.26	1.3	347.14	1.3	10535	40.2	9783	37.3	15698	59.8	16450	62.7
Pangdo	16425	345.24	2.1	339.90	2.1	8666	52.7	8242	50.2	7762	47.3	8184	49.8
Tangga	20152	348.12	1.7	342.27	1.7	10081	50.0	9432	46.8	10071	50.0	10720	53.2
Yangbajain	2645	316.31	12.0	278.26	10.5	1352	51.1	946	35.8	1293	48.9	1699	64.2

641

642 **Table 4.** Mann-Kendall trend test with trend-free pre-whitening of annual mean air temperature (°C), precipitation (mm) and streamflow (mm) in
643 four catchments of the Lhasa River Basin

	Air temperature		Precipitation		Streamflow	
	Z_C	β (°C/a)	Z_C	β (mm/a)	Z_C	β (mm/a)
Lhasa	6.07**	0.028	1.16	1.581	1.09	1.420
Pangdo	6.19**	0.026	0.89	1.435	0.30	0.223
Tangga	7.35**	0.021	1.48	2.005	-0.62	-0.531
Yangbajain	4.48**	0.028	1.28	2.541	2.07*	1.230

644

Figure captions

Figure 1. (a) The location, (b) elevation and glacier distribution for the twice Chinese Glacier Inventory, only the location of glacier snouts in 1960 were provided in the First Chinese Glacier Inventory, and the boundaries of glaciers were shown in the Second Chinese Glacier Inventory, and (c) twice maps of frozen ground distribution (Li and Cheng, 1996; Zou et al., 2017) in the Yangbajain Catchment.

Figure 2. Seasonal variation of streamflow (*R*), mean air temperature (*T*), and precipitation (*P*) in the Yangbajain Catchment.

Figure 3. Diagram depicting the changes of surface water, groundwater and active groundwater storage due to glacier melt and permafrost thawing under (a) past climate and (b) warmer climate.

Figure 4. Variations of annual (a) streamflow and (b) baseflow from 1979 to 2013.

Figure 5. Variations of annual (a) mean air temperature and (b) precipitation from 1979 to 2013.

Figure 6. Variations of seasonal streamflow and baseflow in (a) spring, (b) summer, (c) autumn, and (d) winter from 1979 to 2013.

Figure 7. Variations of seasonal mean air temperature in (a) spring, (b) summer, (c) autumn, and (d) winter from 1979 to 2013.

Figure 8. Recession data points of $-dy/dt$ versus y and fitted recession curves by decades in log-log space. The black point line, dotted line, and solid line represent recession curves in the 1980s, 1990s, and 2000s, respectively.

666 **Figure 9.** Variations of (a) the recession coefficient *K* and (b) the estimated
667 groundwater storage *S* from 1979 to 2013 and the estimated groundwater storage
668 changes from 2003 to 2015 by GRACE data.

669 **Figure 10.** Variations of annual NDVI from 1998 to 2013 in the catchment.

670 **Figure 11.** The total area and volume of glaciers in the Yangbajain Catchment in 1960
671 and 2009.

672

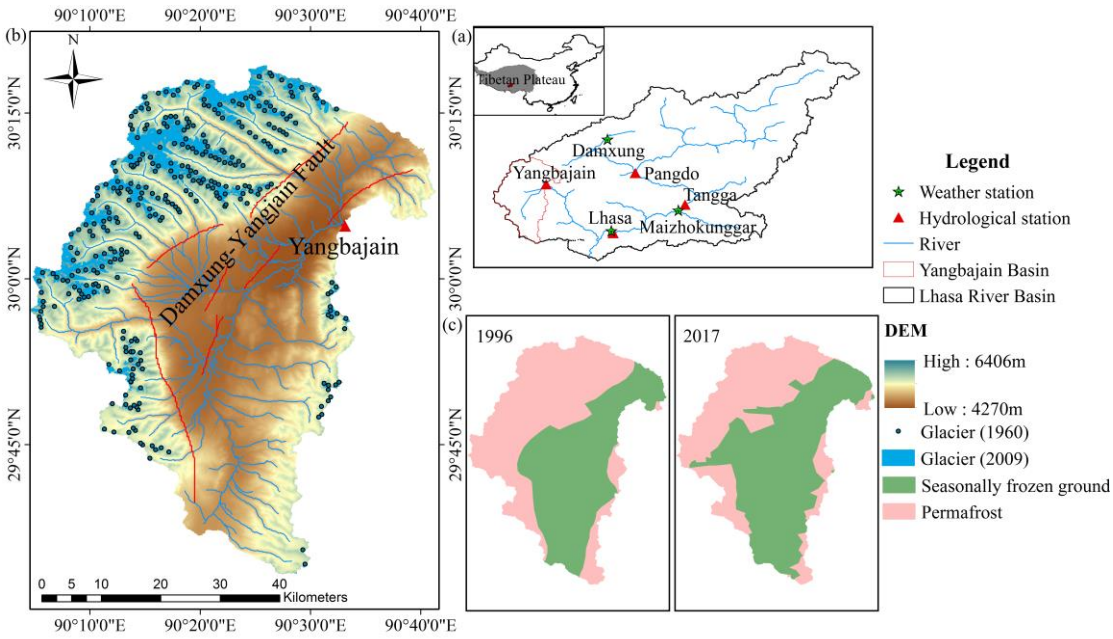

673

674 **Figure 1.** (a) The location, (b) elevation and glacier distribution for the twice Chinese

675 Glacier Inventory, only the location of glacier snouts in 1960 were provided in the

676 First Chinese Glacier Inventory, and the boundaries of glaciers were shown in the

677 Second Chinese Glacier Inventory, and (c) twice maps of frozen ground distribution

678 (Li and Cheng, 1996; Zou et al., 2017) in the Yangbajain Catchment.

679

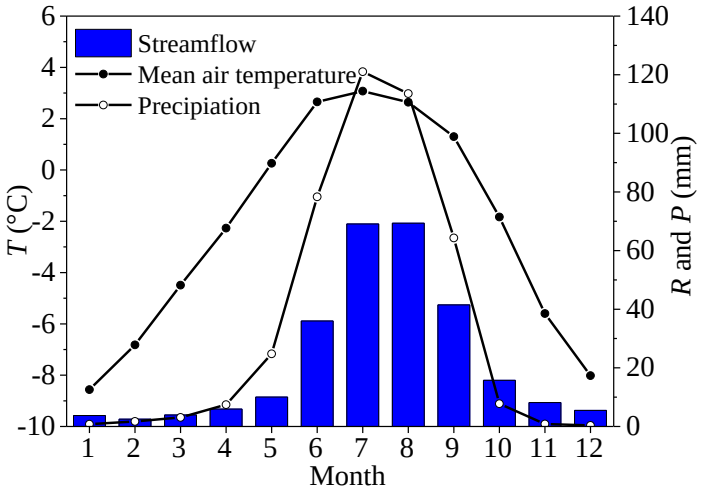

680

681 **Figure 2.** Seasonal variation of streamflow (*R*), mean air temperature (*T*), and

682 precipitation (*P*) in the Yangbajain Catchment.

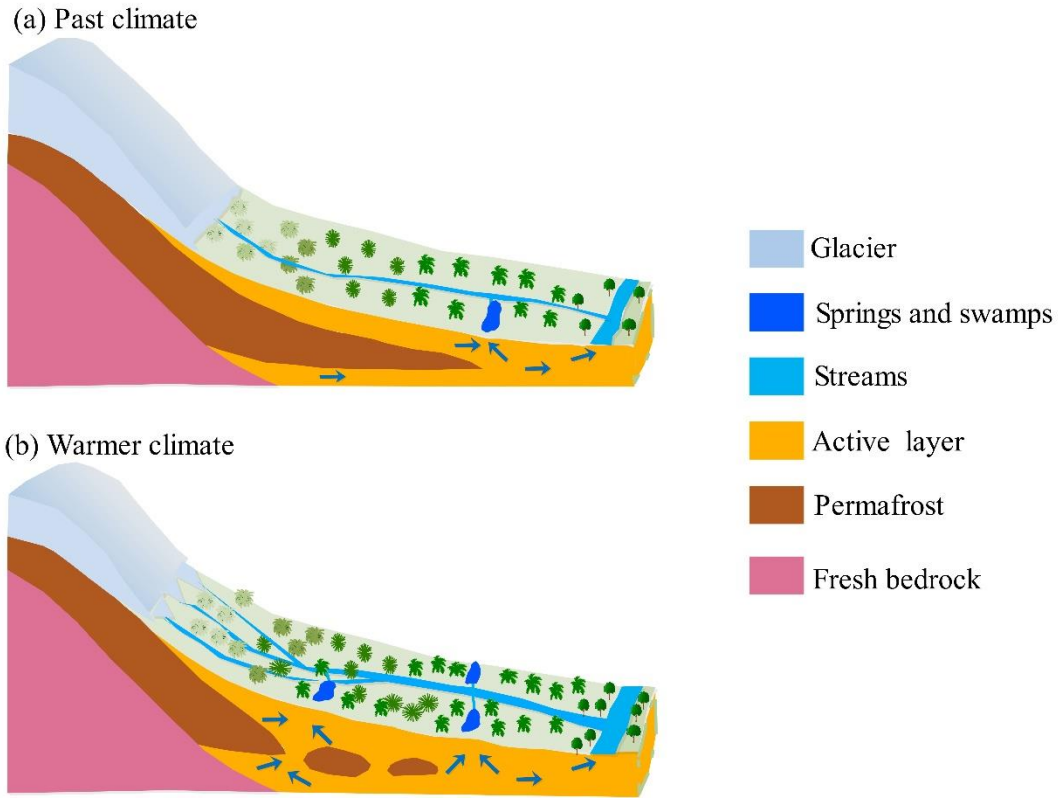

683

684 **Figure 3.** Diagram depicting the changes of surface water, groundwater and active

685 groundwater storage due to glacier melt and permafrost thawing under (a) past climate

686 and (b) warmer climate.

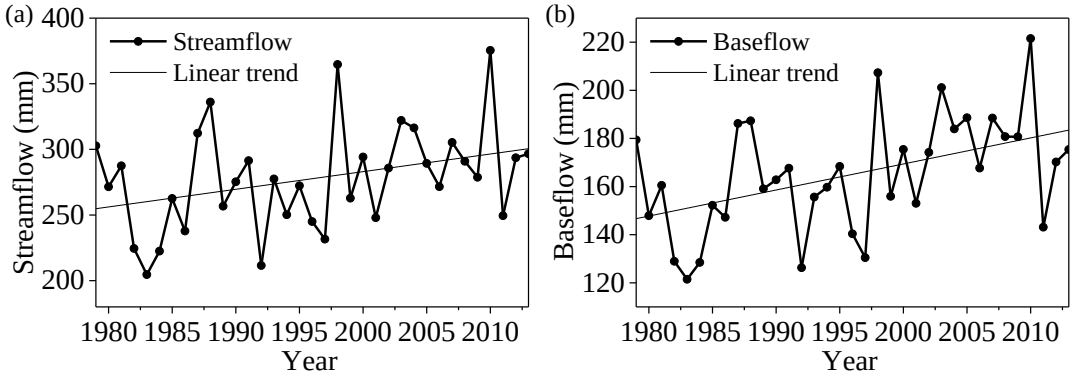

687

688 **Figure 4.** Variations of annual (a) streamflow and (b) baseflow from 1979 to 2013.

689

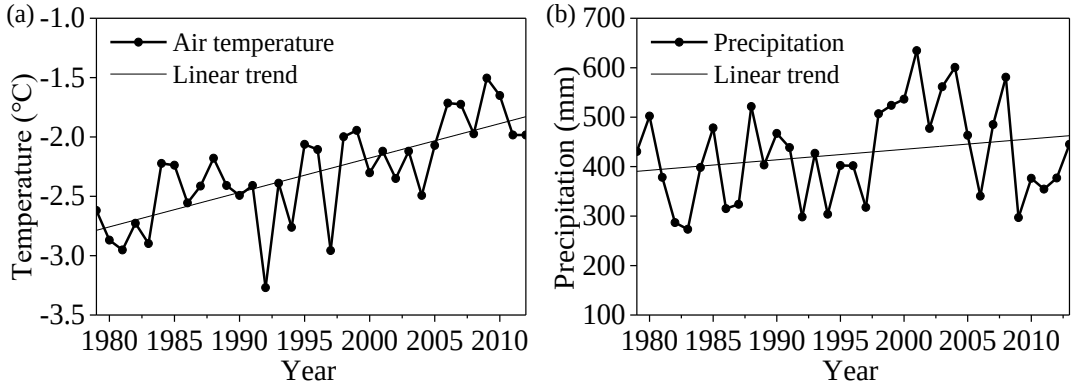

690

691 **Figure 5.** Variations of annual (a) mean air temperature and (b) precipitation from

692 1979 to 2013.

693

694

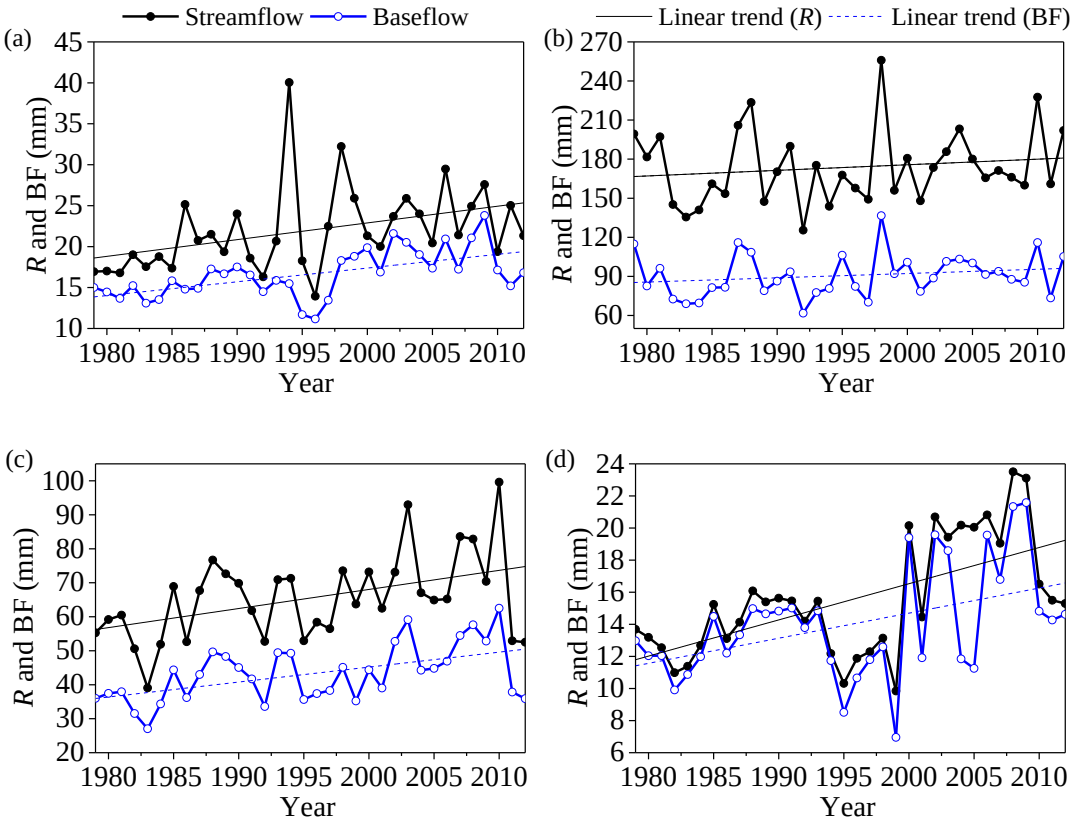

695

696 **Figure 6.** Variations of seasonal streamflow and baseflow in (a) spring, (b) summer,

697 (c) autumn, and (d) winter from 1979 to 2013.

698

699

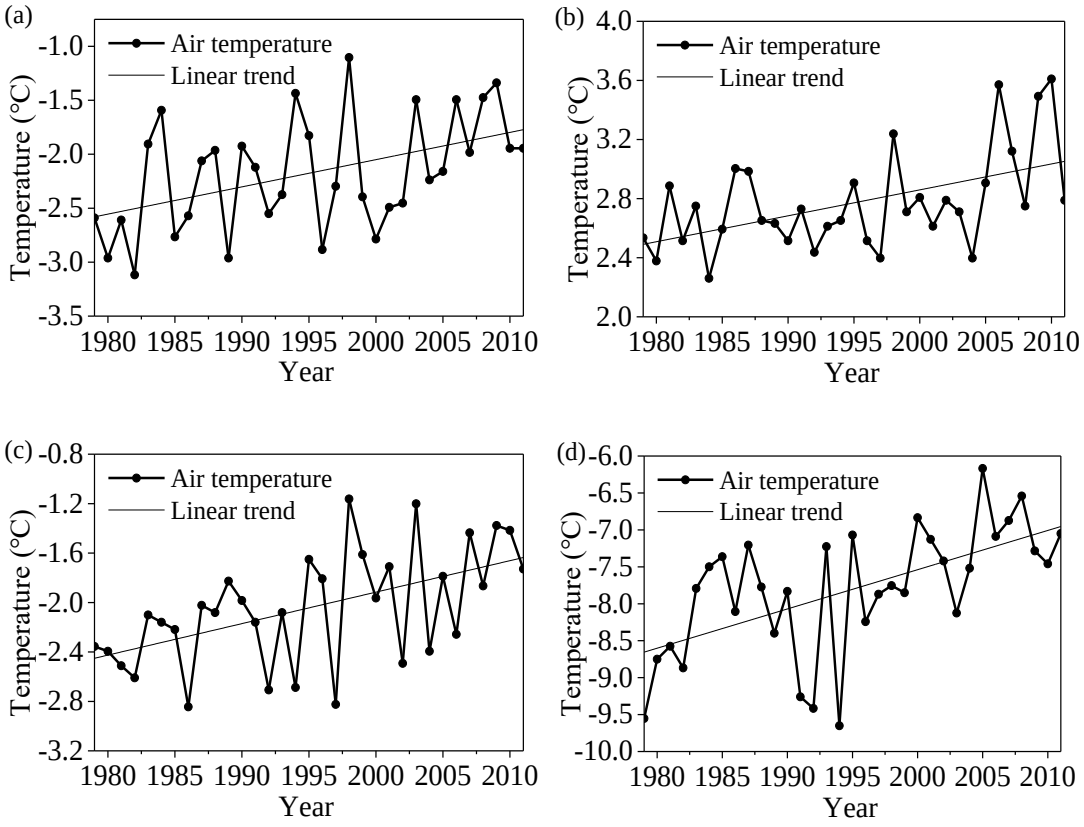

700

701 **Figure 7.** Variations of seasonal mean air temperature in (a) spring, (b) summer, (c)

702 autumn, and (d) winter from 1979 to 2013.

703

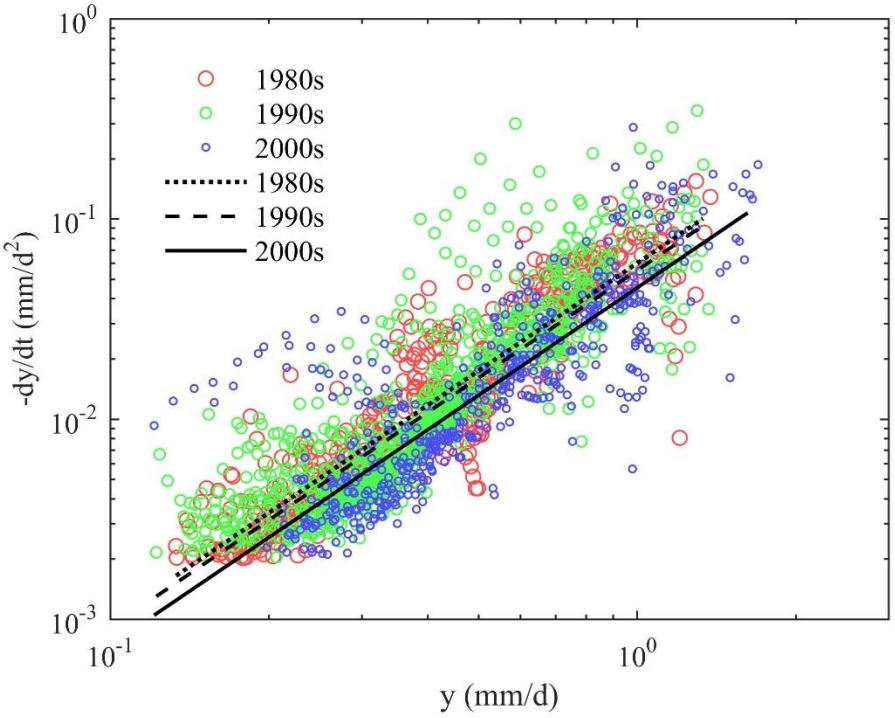

Figure 8. Recession data points of *-dy/dt* versus *y* and fitted recession curves by decades in log-log space. The black point line, dotted line, and solid line represent recession curves in the 1980s, 1990s, and 2000s, respectively.

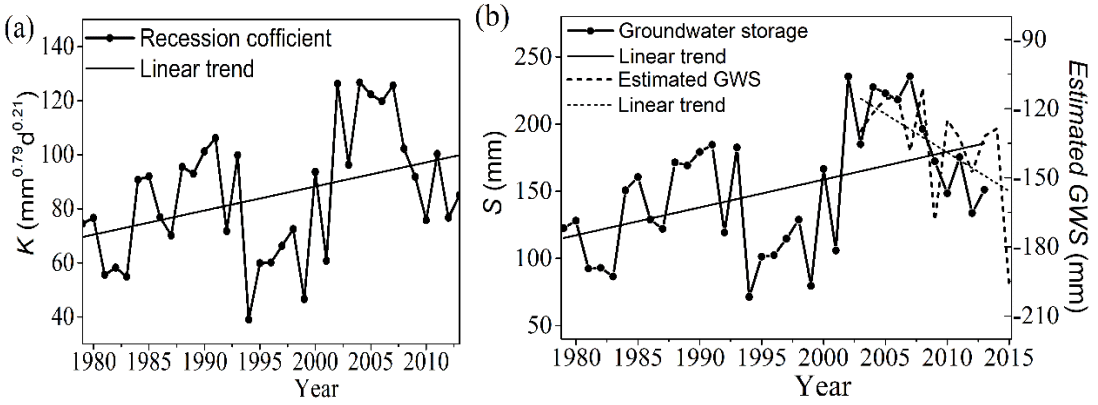

Figure 9. Variations of (a) the recession coefficient *K* and (b) the estimated groundwater storage *S* from 1979 to 2013 and the estimated groundwater storage changes from 2003 to 2015 by GRACE data.

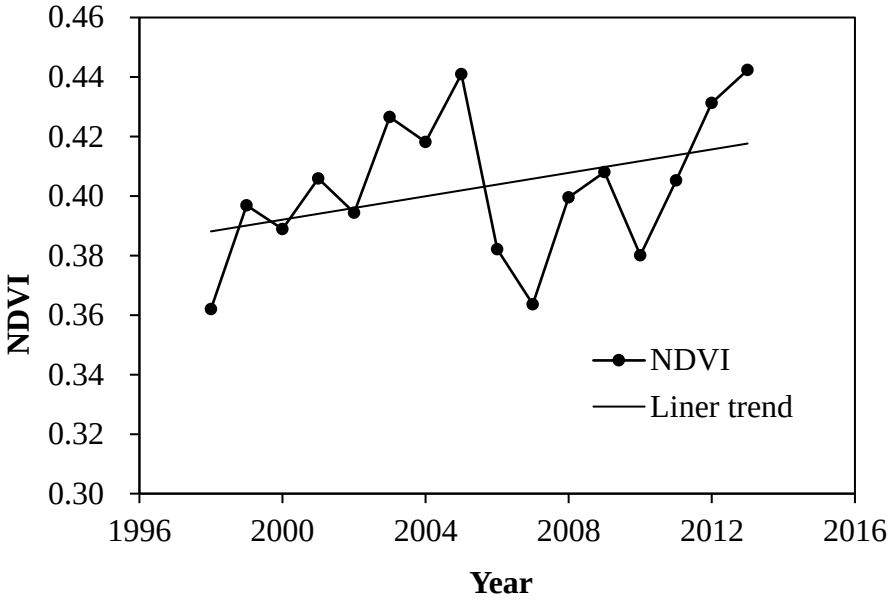

714

715 **Figure 10.** Variations of annual NDVI from 1998 to 2013 in the catchment.

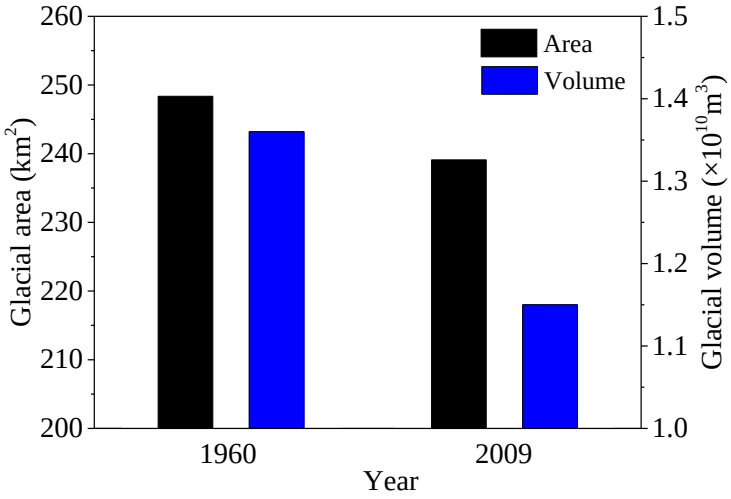

716

717 **Figure 11.** The total area and volume of glaciers in the Yangbajain Catchment in 1960

718 and 2009.

719